Available online at www.sciencedirect.com
ScienceDirect
Journal of Pharmaceutical and Biomedical Analysis 43 (2007) 330–334
JOURNAL OF PHARMACEUTICAL AND BIOMEDICAL ANALYSIS
www.elsevier.com/locate/jpba

Short communication

Studies on the interactions between DNA and PAMAM with fluorescent probe $[Ru(phen)_2dppz]^{2+}$

Linzhu Zhou [a], Lu Gan [a], Haibing Li [b], Xiangliang Yang [a,*]

[a] College of Life Science and Technology, Huazhong University of Science and Technology, Wuhan 430074, PR China
[b] Chemistry Department, Huazhong Normal University, Wuhan 430079, PR China

Received 14 April 2006; received in revised form 8 June 2006; accepted 9 June 2006
Available online 26 July 2006

Abstract

The interactions between plasmid DNA and cationic polymers are of interest for their potential biological applications. In this paper, the interactions of DNA with polyamidoamine (PAMAM) dendrimer were studied by fluorescence spectroscopy and stopped-flow technique. A rapid and reproducible fluorescent assay method had been developed for assessing PAMAM and DNA interactions using $[Ru(phen)_2dppz]^{2+}$ as a probe. We further studied the kinetics of PAMAM binding to DNA and the reverse process of DNA dissociation from the complexes. The results indicated that DNA condensation was the rate-determining step during the complexation process, while DNA unfolding and expansion was the rate-determining step during the DNA dissociation process. At N/P ratios before reaching the thermodynamically most stable state, the complexes of DNA and PAMAM were incompact and could dissociate to some extent. And at N/P ratios above 2.0, DNA was fully condensed by PAMAM and dissociation was increasingly difficult. These results provided some useful instructions for self-assembling and disassembling of DNA as well as efficient gene delivery applications.
© 2006 Elsevier B.V. All rights reserved.

Keywords: Polyamidoamine (PAMAM); DNA; Interactions; Association; Dissociation; Stopped-flow; $[Ru(phen)_2dppz]^{2+}$

1. Introduction

The development of efficient and safe gene delivery carriers that can transfer DNA into the nuclei of target cells is a key factor for success of gene therapy [1]. Polyamidoamine (PAMAM) dendrimers are a class of nanoscopic polymers with highly branched spherical structure and a unique surface of primary amines as well as tertiary amines at branch points. PAMAM can transport DNA into a large variety of cell types and have emerged as a promising non-viral gene carrier for genetic medicines due to their safety and efficiency [2–6].

The cationic polymers spontaneously assemble with DNA to form net positively charged compact complexes. This process consists of at least two sequential steps: the first is electrostatic binding between positively charged polymers and negatively charged phosphate backbone, the second is DNA condensation driven by local and eventually long-range charge neutralization [7]. DNA in these complexes appears to organize into rod-like or toroidal structures with an underlying square or hexagonal unit cell depending on the chemistry of polycation and charge ratio of polycation to DNA [6,8]. The precondensation of transgenic DNA in vitro plays an important role in cellular uptake, endosomal escape and cytoplasmic delivery, whereas the prerequisite for DNA to exert its activity is to release from the carriers to be read by the host transcriptional machinery [9,10]. It would be desirable to have complete DNA uncoating before delivery into the nucleus. However, the dissociation of DNA from a cationic polymer is usually restricted by the driving forces that contribute to efficient DNA condensation [11–13]. Recently, it has been proved that complexes of DNA and cationic peptides can dissociate in vitro and irreversible association can take place under certain conditions [14,15]. Because of the potential importance of such studies in gene transfer, we have become interested in the processes of DNA condensation and its reverse process in order to achieve more effective gene delivery applications.

In the present work, we used fluorescence spectroscopy and stopped-flow kinetic analysis to characterize the interactions between DNA and PAMAM probed by $[Ru(phen)_2dppz]^{2+}$.

* Corresponding author. Tel.: +86 27 87794520; fax: +86 27 87794517.
E-mail address: yangxl@mail.hust.edu.cn (X. Yang).

0731-7085/$ – see front matter © 2006 Elsevier B.V. All rights reserved.
doi:10.1016/j.jpba.2006.06.021

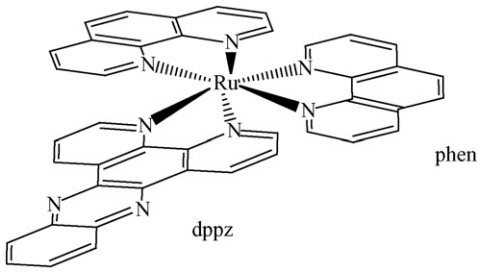

Fig. 1. Structure of $[Ru(phen)_2dppz]^{2+}$.

The commonly used DNA dyes include minor groove binding dyes (Hoechst 33258, DAPI) and intercalating dyes (EtBr, YOYO-1). The fluorescence of dyes with DNA is altered as a result of environmental changes in DNA minor groove or displacement from their binding sites by polycations [16]. The $[Ru(phen)_2dppz]^{2+}$ (phen = 1,10-phenanlinthroline; dppz = dipyrido[3,2-a:2′,3′-c]phenazine, structure shown in Fig. 1) is a molecular light switching compound that has no photoluminescence in aqueous solution but displays intense photoluminescence when intercalating into the double-helical DNA with the extended dppz ligand [17,18]. This study took advantage of the unique property of $[Ru(phen)_2dppz]^{2+}$ and used it as a substitute for ethidium bromide for its safety and sensitivity.

2. Experimental

2.1. Materials

PAMAM (polyamidoamine dendrimer, Generation 5.0) was obtained from Aldrich. $[Ru(phen)_2dppz]^{2+}$ was a gift from Prof. Zhike He (Wuhan University, China). $pVIVO_2$-GFP/LacZ was obtained from Invitrogen. The plasmid was amplified in *E. coli* (strain DH5α) and purified by column chromatography. The concentration and purity of plasmid were determined by UV spectroscopy. Agarose gel (0.7%) electrophoretic analysis showed that the plasmid was mainly in supercoiled form.

2.2. Displacement and exclusion assays

In the displacement assay, DNA and $[Ru(phen)_2dppz]^{2+}$ solutions were mixed in TE buffer (10 mM Tris, 1 mM EDTA, pH 7.8) and allowed to equilibrate for 1 min. Then, appropriate amounts of PAMAM were added to the solution and mixed to obtain the desired N/P ratios (the N/P ratio was based on the calculation of the electrostatic charge present on each component, i.e. the number of terminal NH_2 groups on PAMAM to the number of phosphate groups on the nucleic acid). The fluorescence was measured after 1 min equilibration.

In the exclusion assay, DNA and varying masses of PAMAM (dependent on the N/P ratio required) were mixed together in TE buffer and allowed to incubate at room temperature for 30 min. Immediately prior to analysis, $[Ru(phen)_2dppz]^{2+}$ solution was added. The sample was mixed sufficiently and the fluorescence was measured.

The final concentrations of DNA and $[Ru(phen)_2dppz]^{2+}$ in both assays were 1 μg/ml and 1.5×10^{-6} M, respectively. The fluorescence was measured with a HITACHI F-4500 fluorescence spectrometer ($\lambda_{excitation} = 453$ nm, $\lambda_{emission} = 598$ nm). All samples were prepared in triplicate and the fluorescence was expressed with the following equation Eq. (1):

$$\text{relative fluorescence intensity} \frac{F_{obs} F_0}{F_{DNA} F_0} \quad (1)$$

where F_{obs}, F_0, and F_{DNA} were the fluorescence intensities of a given sample, $[Ru(phen)_2dppz]^{2+}$ in buffer alone, and $[Ru(phen)_2dppz]^{2+}$ bound to DNA in the absence of PAMAM competition for binding.

2.3. Binding and dissociation kinetic analyses

The binding and dissociation of DNA and PAMAM were carried out with an SX-18MV stopped-flow fluorimeter setup (Applied Photophysics Ltd., UK). In the binding kinetic analysis, DNA and $[Ru(phen)_2dppz]^{2+}$ solutions were mixed in TE buffer and allowed to equilibrate for 1 min. Then, the DNA–$[Ru(phen)_2dppz]^{2+}$ complexes and PAMAM (with different concentrations) were enclosed into the syringes, respectively, pushed quickly to the mixing vessel and stopped flowing suddenly. While in the dissociation kinetic analysis, DNA and varying masses of PAMAM (dependent on the N/P ratio required) were mixed together in TE buffer and allowed to incubate at room temperature for 30 min. Then, the $[Ru(phen)_2dppz]^{2+}$ solution and PAMAM–DNA complexes were enclosed into the syringes and the stopped-flow experiments were carried out accordingly. The fluorescence was collected on excitation at 453 nm using a cutoff filter at 515 nm. The final concentrations of DNA and $[Ru(phen)_2dppz]^{2+}$ were 3 μg/ml and 4.5×10^{-6} M, respectively. All experiments were carried out in six times and performed in TE buffer at 25 °C.

Data analysis was performed using the Sigmaplot software. The association kinetic traces were fit by a double exponential decay function Eq. (2) and the dissociation kinetic traces were fit by a double exponential growth function Eq. (3):

$$yy_0 A_1 \, e^{k_1 t} A_2 \, e^{k_2 t} \quad (2)$$

$$yy_0 A_1 (1e^{k_1 t}) A_2 (1e^{k_2 t}) \quad (3)$$

3. Results and discussion

3.1. Displacement and exclusion assays

The displacement and exclusion assays employing a fluorescent probe are commonly used to characterize the interactions between DNA and gene delivery carriers [19]. The ability of PAMAM to displace or exclude $[Ru(phen)_2dppz]^{2+}$ from DNA was shown in Fig. 2. As the concentrations of PAMAM were increased, the fluorescence intensity of $[Ru(phen)_2dppz]^{2+}$/DNA complexes decreased until a minimum level was reached close to baseline fluorescence. At charge ratios above 2, PAMAM displaced or excluded over 90% of the dye.

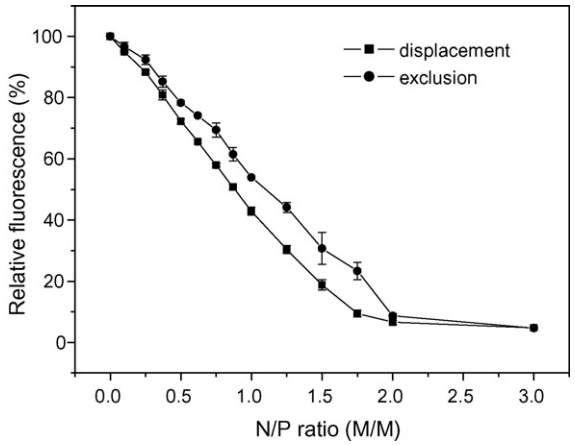

Fig. 2. $[Ru(phen)_2dppz]^{2+}$ displacement and exclusion assays of PAMAM. (■) Displacement assay, 2 μg of DNA in 1.7 ml TE buffer (10 mM Tris, 1 mM EDTA, pH 7.8) was mixed with 0.3 ml $[Ru(phen)_2dppz]^{2+}$ solution (10^{-5} M). Appropriate amounts of PAMAM (0.6 mM) were added and the fluorescence determined after 1 min equilibration ($n = 3$). (●) Exclusion assay, 2 μg of DNA was mixed with appropriate amounts of PAMAM in TE buffer and incubated for 30 min. Prior to analysis, 0.3 ml $[Ru(phen)_2dppz]^{2+}$ solution (10^{-5} M) was added. Each solution was then diluted to 2 ml with TE buffer and the fluorescence measured ($n = 3$). The final concentrations of DNA and $[Ru(phen)_2dppz]^{2+}$ in both assays were 1 μg/ml and 1.5×10^{-6} M, respectively. The fluorescence was measured on excitation at 453 nm and emission at 598 nm.

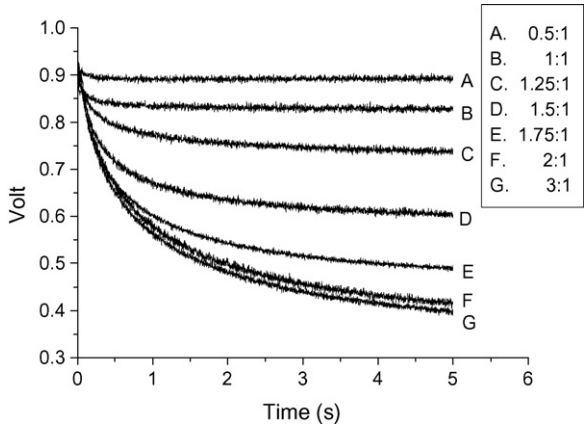

Fig. 3. Kinetic traces for binding of PAMAM to DNA (the N/P ratio was indicated in the legend). Varying masses of PAMAM were mixed isometrically with DNA–$[Ru(phen)_2dppz]^{2+}$ complexes. The final concentrations of DNA and $[Ru(phen)_2dppz]^{2+}$ were 3 μg/ml and 4.5×10^{-6} M, respectively. The fluorescence was collected on excitation at 453 nm using a cutoff filter at 515 nm. All experiments were carried out in six times and performed in TE buffer (10 mM Tris, 1 mM EDTA, pH 7.8) at 25 °C.

The N/P ratio corresponding to minimum fluorescence was about 2.0, meaning that excess positive charges were required for complete neutralization of the DNA negative charges. This was likely due to incomplete protonation of the amine groups on PAMAM under the conditions employed (pH 7.8) since the degree of protonation is pH dependent [20–22]. The stoichiometric charge ratio at a lower pH would be under 2.0 as expected from a higher degree of protonation. For a certain N/P ratio, the relative fluorescence intensity derived from displacement assay was slightly lower than that from exclusion assay. This small difference was mainly due to the competition of binding and dissociation between DNA and PAMAM. In the displacement assay, PAMAM was added to DNA and the binding effect was dominant. While in the exclusion assay, DNA and PAMAM formed complexes and $[Ru(phen)_2dppz]^{2+}$ was added afterwards. The complexes were diluted to follow dissociation by competition of the probe, and the dissociated DNA was responsible for the additional fluorescence intensity.

3.2. Binding kinetic analysis

Binding kinetic experiments of PAMAM and DNA (with $[Ru(phen)_2dppz]^{2+}$) at various N/P ratios were performed to monitor complex formation and DNA condensation (Fig. 3). The binding of PAMAM to DNA resulted in charge neutralization, DNA condensation and subsequent exclusion of $[Ru(phen)_2dppz]^{2+}$. The decrease of fluorescence intensity increased with the increase of PAMAM concentration until saturation was achieved at N/P ratio of 2.0.

The binding kinetic traces were fit with a double exponential decay function to get two association rate constants (k_1 and k_2) and fluorescence amplitudes (A_1 and A_2) (Fig. 4). Since the association and dissociation of $[Ru(phen)_2dppz]^{2+}$ with DNA occurred within the dead-time of mixing, the two association rates were $[Ru(phen)_2dppz]^{2+}$ exclusion rates that actually corresponded to the two phases during complex for-

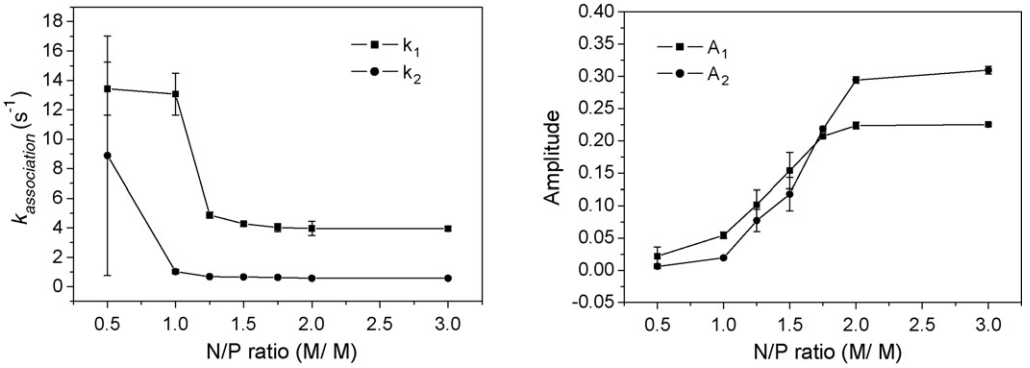

Fig. 4. Association rate constants and fluorescence amplitudes of $[Ru(phen)_2dppz]^{2+}$ exclusion following the binding of PAMAM to DNA. The values of rate and amplitude 1 (■) and rate and amplitude 2 (●) were obtained from the fitting of the binding kinetic traces to a double exponential decay function and plotted as a function of N/P ratios. Six experiments were averaged for each N/P ratio. Error bars show the standard deviation.

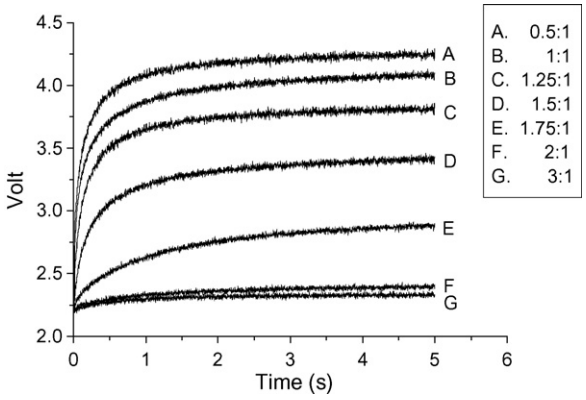

Fig. 5. Kinetic traces for dissociation of PAMAM/DNA complexes (the N/P ratio was indicated in the legend). Varying amounts of PAMAM were mixed with DNA and allowed to incubate 30 min. The mixture was then mixed isometrically with $[Ru(phen)_2dppz]^{2+}$ on-line. The final concentrations of DNA and $[Ru(phen)_2dppz]^{2+}$ were 3 μg/ml and 4.5×10^{-6} M, respectively. The fluorescence was collected on excitation at 453 nm using a cutoff filter at 515 nm. All experiments were carried out in six times and performed in TE buffer (10 mM Tris, 1 mM EDTA, pH 7.8) at 25 °C.

mation described earlier (PAMAM binding and DNA condensation, respectively). The association rate constants were found to decrease with the increase of PAMAM concentration for N/P ratios below 2.0. Moreover, k_1 was larger than k_2 indicating that DNA condensation was the rate-determining step. In addition, the fluorescence amplitudes were found to increase with the increase of PAMAM concentration at lower N/P ratios, and then stabilized at ratios above 2.0, indicating the maximum DNA condensation and $[Ru(phen)_2dppz]^{2+}$ exclusion. PAMAM and DNA formed stable complexes under these conditions.

3.3. Dissociation kinetic analysis

Dissociation experiments of PAMAM/DNA complexes were performed by mixing the complexes with $[Ru(phen)_2dppz]^{2+}$ to follow the increase in fluorescence intensity (Fig. 5). Following addition of the fluorescent probe, PAMAM/DNA complexes were diluted to obtain the dissociation kinetics by the competition of $[Ru(phen)_2dppz]^{2+}$ for binding to DNA. The dissociated DNA tended to rearrange, $[Ru(phen)_2dppz]^{2+}$ intercalated to DNA base pair and fluoresced. In addition, the recovered fluorescence decreased with the increase of N/P ratios.

The dissociation kinetic traces were fit with a double exponential growth function to get two dissociation rate constants (k_1 and k_2) and fluorescence amplitudes (A_1 and A_2) (Fig. 6). The two dissociation rates were $[Ru(phen)_2dppz]^{2+}$ inclusion rates that related to the two phases during complex dissociation, namely the dissociation of DNA from the complexes and accompanied structural rearrangement (unfolding and expansion), respectively. The dissociation rate constants decreased with the increase of PAMAM concentration for N/P ratios below 2.0. And k_1 was much larger than k_2 indicating that DNA expansion was the rate-determining step. The fluorescence amplitudes were found to decrease with the increasing N/P ratios and stabilized at ratios above 2.0, indicating that the complex dissociation and DNA expansion was increasingly difficult. As the PAMAM concentration was increased to a certain degree, PAMAM and DNA formed thermodynamically stable complexes and the external forces were less efficient to destroy the compact structures.

Studies have shown that DNA condensation is a readily reversible process under certain conditions [14,15]. At charge ratios before reaching the fully condensed point, the complexes were incompact and could dissociate to a certain extent. And with increasing amounts of cationic carriers, the complexes became increasingly stable and dissociation was restricted by the driving forces that contributed to efficient DNA condensation [11–13]. These results were completely consistent with our dissociation kinetic data. In the absence of changes in environmental conditions (e.g. pH, ionic strength or temperature), dissociation of DNA from cationic carriers presented a significant challenge [23,24]. Since DNA must be released from the complexes just prior to nuclear entry, the inefficiency of dissociation has emerged as a factor limiting the effectiveness of cationic gene delivery carriers. The fully condensed DNA was likely to inhibit transcription due to the impossibility of intracellular dissociation.

Despite the limitations on complex dissociation, since PAMAM was a kind of biodegradable polymers, it was speculated that the hydrolysis of the ester functionality in PAMAM

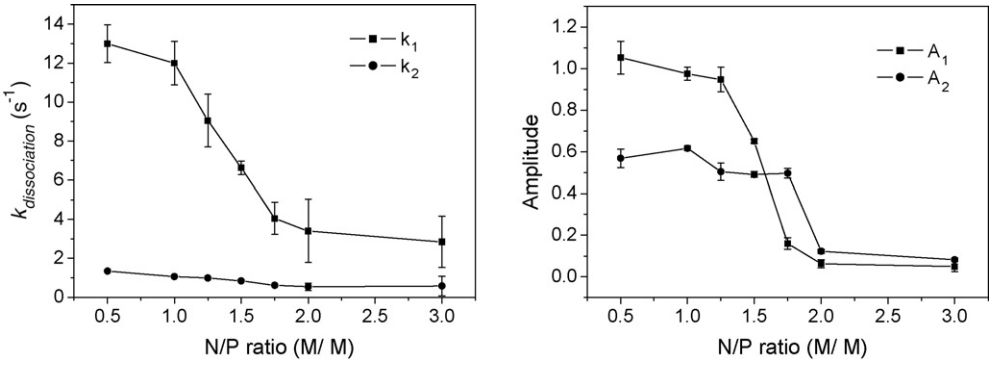

Fig. 6. Dissociation rate constants and fluorescence amplitudes of $[Ru(phen)_2dppz]^{2+}$ inclusion following the dissociation of PAMAM/DNA complexes. The values of rate and amplitude 1 (■) and rate and amplitude 2 (●) were obtained from the fitting of the dissociation kinetic traces to a double exponential growth function and plotted as a function of N/P ratios. Six experiments were averaged for each N/P ratio. Error bars show the standard deviation.

under physiological conditions would result in a gradual reduction in positive charge density and a consequential change in the electrostatic interactions between DNA and PAMAM. Therefore, it was possible to facilitate the dissociation of DNA from the complexes as time went on. In addition, some negatively charged components in vivo might have chance to compete with DNA for binding to the cationic carriers so that DNA could release from the complexes [25]. These arguments provided some helpful insights into the efficient gene delivery. Attempts to examine the dissociation of DNA from PAMAM over a broad range of times and to synthesize new carriers that can promote the dissociation more effectively are currently in progress in our laboratory.

4. Conclusions

This work presented some useful insights into DNA condensation by PAMAM and dissociation of PAMAM/DNA complexes. The use of $[Ru(phen)_2dppz]^{2+}$ had provided us with a safe and feasible method to characterize the interactions between DNA and PAMAM. Complexes formed under intermediate ratios were relatively incompact. While at higher ratios above 2.0, DNA was fully condensed by PAMAM and dissociation was progressively less efficient, which was consistent with the formation of thermodynamically more stable forms. With the better understanding of DNA condensation and the reverse dissociation process, we were capable of promoting the delivery and/or release of DNA more efficiently in gene therapy applications.

Acknowledgments

Prof. Zhike He is greatly acknowledged for providing the fluorescent probe $[Ru(phen)_2dppz]^{2+}$. And we thank Prof. Ruxiu Cai for having kindly reread our manuscript. This work was supported by a grant of the National 863 project of China (no. 2004AA2Z3212) and Chenguang Project of Wuhan city (no. 20055003059-42).

References

[1] C.M. Wiethoff, C.R. Middaugh, J. Pharm. Sci. 92 (2003) 203–217.
[2] J.F. Kukowska-Latallo, A.U. Bielinska, J. Johnson, R. Spindler, D.A. Tomalia, J.R. Baker Jr., Proc. Natl. Acad. Sci. U.S.A. 93 (1996) 4897–4902.
[3] J. Dennig, E. Duncan, Rev. Mol. Biotech. 90 (2002) 339–347.
[4] M. El-Sayed, M. Ginski, C. Rhodes, H. Ghandehari, J. Control. Rel. 81 (2002) 355–365.
[5] C.S. Braun, J.A. Vetro, D.A. Tomalia, G.S. Koe, J.G. Koe, C.R. Middaugh, J. Pharm. Sci. 94 (2005) 423–436.
[6] A.U. Bielinska, J.F. Kukowska-Latallo, J.R. Baker Jr., Biochim. Biophys. Acta 1353 (1997) 180–190.
[7] C.S. Braun, M.T. Fisher, D.A. Tomalia, G.S. Koe, J.G. Koe, C.R. Middaugh, Biophys. J. 88 (2005) 4146–4158.
[8] H.M. Evans, A. Ahmad, K. Ewert, T. Pfohl, A. Martin-Herranz, R.F. Bruinsma, C.R. Safinya, Phys. Rev. Lett. 91 (2003) 075501.
[9] J. Zabner, A.J. Fasbender, T. Moninger, K.A. Poellinger, M.J. Welsh, J. Biol. Chem. 270 (1995) 18997–19007.
[10] C.W. Pouton, L.W. Seymour, Adv. Drug Deliv. Rev. 46 (2001) 187–203.
[11] W.T. Godbey, K.K. Wu, A.G. Mikos, Proc. Natl. Acad. Sci. U.S.A. 96 (1999) 5177–5181.
[12] R. Kircheis, L. Wightman, E. Wagner, Adv. Drug Deliv. Rev. 53 (2001) 341–358.
[13] J. Suh, D. Wirtz, J. Hanes, Proc. Natl. Acad. Sci. U.S.A. 100 (2003) 3878–3882.
[14] M. Keller, T. Tagawa, M. Preuss, A.D. Miller, Biochemistry 41 (2002) 652–659.
[15] M. Tecle, M. Preuss, A.D. Miller, Biochemistry 42 (2003) 10343–10347.
[16] C.M. Wiethoff, M.L. Gill, G.S. Koe, J.G. Koe, C.R. Middaugh, J. Pharm. Sci. 92 (2003) 1272–1285.
[17] E. Amouyal, A. Homsi, J.C. Chambron, J.P. Sauvage, J. Chem. Soc., Dalton Trans. 6 (1990) 1841–1845.
[18] L. Ling, G. Song, Z. He, H. Liu, Y. Zeng, Microchem. J. 63 (1999) 356–364.
[19] A.J. Geall, I.S. Blagbrough, J. Pharm. Biomed. Anal. 22 (2000) 849–859.
[20] W. Chen, N.J. Turro, D.A. Tomalia, Langmuir 16 (2000) 15–19.
[21] W. Chen, D.A. Tomalia, N.J. Turro, Macromolecules 33 (2000) 9169–9172.
[22] D. Cakasa, J. Kleimann, M. Borkovec, Macromolecules 36 (2003) 4201–4207.
[23] E. Wagner, Pharm. Res. 21 (2004) 8–14.
[24] X. Liu, J.W. Yang, A.D. Miller, E.A. Nack, D.M. Lynn, Macromolecules 38 (2005) 7907–7914.
[25] O. Zelphati, F.C. Szoka Jr., Proc. Natl. Acad. Sci. U.S.A. 93 (1996) 11493–11498.